University of Copenhagen

Niels Bohr Institute

Center for Quantum Devices

Bachelor's Thesis

Measuring Fractional Quantum Hall Effect

Authors:
Katrine Rasmussen
Christian J. S. Olsen

Supervisor:
Charles M. Marcus

June 12, 2013

Katrine Rasmussen
Januar 25, 1989

Christian J. S. Olsen
August 23, 1988

Acknowledgments

For nearly one year we have been a part of Center for Quantum Devices (QDev). It has been a very awarding and educational year and truly a great introduction to the work of an experimentalist in the field of quantum transport and information. From day one we have felt like a part of QDev. We have enjoyed the great luxury of having so many bright-headed fellow researchers all willing to help us.

We would like to express our deep gratitude to Charles M. Marcus for giving us the opportunity to come and work in QDev and entrusting us with a cryofree dilution refrigerator, we feel very privileged. Also we would like to thank C. M. Marcus for taking the time to educate us in the complex theory of fractional quantum Hall effect and its possible application in building a topological quantum computer.

We owe a sincere thanks to Ferdinand Kümmeth for his patience in answering our countless questions and helping us setting up a cryofree dilution refrigerator.

We have benefitted greatly from our mail correspondence with Douglas T. McClure, a former researcher in the fractional quantum Hall physics from the old Marcus lab. Through our correspondence Douglas has helped us understanding our measurements and how to analyze our data.

Andrew Higginbotham and Willy Chang have both been a great source of knowledge and help with daily lab business.

We would like to thank Anders Jellinggaard and Shivendra Upadhyay for introducing us to working in the clean room and helping us with making our UV-lithography work. Furthermore we would like to thank Anders for his patience in helping us with Matlab.

Lastly we would like to thank Mark S. Rudner and Ferdinand Kümmeth for taking the time to proofread our thesis.

Abstract

In this thesis we present the process and considerations involved in setting up a cryofree dilution refrigerator for fractional quantum Hall measurements. As an introduction we explain the theory of the classical Hall effect, the integer quantum Hall effect, the fractional quantum Hall effect and the theory of composite fermions.
Subsequently we describe the experimental setup used to measure the fractional quantum Hall effect, from the macroscopic scale of the fridge to the microscopic scale of the device.
We achieved beautiful and cold Hall traces in a GaAs/AlGaAs quantum well confined 2DEG, showing the fragile fractional state of $\nu = 5/2$. From these traces we estimate the electron temperature to be in the range of 15 to 20 mK.

Motivation

Our motivation for investigating the fractional quantum Hall effect is the prediction that the quasiparticles of some fractional quantum Hall states such as $\nu = 5/2$ possess non-abelian statistics, hereby making them possible candidates for realization of a topological quantum computer.
It has been our intention to write this thesis as an introduction to quantum Hall physics and how to realize quantum Hall phenomena with a cryofree dilution refrigerator. The intended reader is that of a fellow bachelor student in physics unfamiliar with the concepts of quantum Hall physics.

Contents

Title page . . . i
Acknowledsments . . . ii
Abstract . . . iii
Motivation . . . iii
Table of Contents . . . iv
List of Figures . . . v

1 Theory **1**
1.1 The Hall Effect . . . 1
1.2 The Quantum Hall Effect . . . 2
1.2.1 Two-Dimensional Electron Systems . . . 2
1.2.2 Quantization . . . 3
1.2.3 Filling Factor . . . 5
1.2.4 Edge States . . . 6
1.2.5 Fractional Quantum Hall Effect . . . 7

2 Setup **11**
2.1 Cryofree Dilution Refrigerator . . . 11
2.2 Heat Sinks . . . 12
2.3 Eddy Currents . . . 13
2.4 Puck . . . 15
2.5 Wiring . . . 15
2.6 Noise Reduction . . . 16
2.7 Data Acquisition . . . 16
2.8 Wafer . . . 18

3 Data **20**
3.1 QHE in a GaAs/AlGaAs QW structure . . . 20
3.2 2DEG temperature . . . 21

4 Conclusion and Outlook **24**

A Sapphire heat sink recipe **25**

B Wafer - P2-22-10.1 **27**

C The effect of high capacitance **28**

D Solidworks design file **29**

Bibliography **30**

List of Figures

1.1 Hall bar and Lorentz force 1
1.2 GaAs/AlGaAs band structure 3
1.3 Degeneracy of Landau levels 5
1.4 Broadening of Landau levels 6
1.5 Skipping-orbit picture and bending of Landau levels 7

2.1 Overview of the fridge 12
2.2 Mixing in the mixing chamber 12
2.3 Bobbin, sapphire heat sinks and signal filters 14
2.4 RC filter and sapphire heat sink 14
2.5 Copper mount 15
2.6 A piece of copper loom 16
2.7 Ground loop 16
2.8 Magnet power supply and the gas handling unit 17
2.9 Device 18

3.1 Hall and longitudinal resistance as a function of magnetic field (0 T - 7 T) 21
3.2 Hall and longitudinal resistance as a function of magnetic field (7 T - 12 T) 22
3.3 Temperature dependence of RIQH and $\nu = 5/2$ 22

B.1 Wafer 27

C.1 The effect of high capacitance 28

Chapter 1

Theory

1.1 The Hall Effect

The Hall effect was discovered in 1879 by Edwin Hall. While running a current I through a sheet of gold leaf, he measured two voltages, one parallel to the current path and one across the current path. He found that when a magnetic field was applied perpendicular to the metal sheet the voltage measured across the sheet V_{xy}, also denoted V_H for Hall voltage, was nonzero[1].
Hall's observation can be understood as the Lorentz force bending the electron paths from the longitudinal direction to the transverse direction, as illustrated with an arrow in figure 1.1. When a perpendicular magnetic field and an in-plane current is applied to a sample of conducting material, it causes an accumulation of negative charge (electrons) on one side of the sample and an equivalent positive charge (excess ions) on the opposite side, in the case of negatively charged carriers. This introduces an electric field in the transverse direction, E_y, see figure 1.1. When the pile up of electrons on the one side of the sample is big enough for E_y to cancel out the Lorentz force due to the magnetic field, the electrons will again on average move in the longitudinal direction[2].
From the Hall voltage one can calculate the Hall resistance[1]:

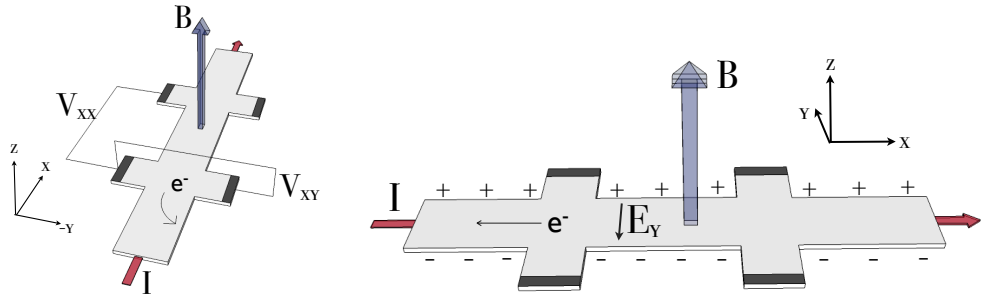

Figure 1.1: *(left) A Hall bar with the current injected in the x-direction (longitudinal). Voltage probes are set up to measure the longitudinal voltage V_{xx} and the Hall voltage V_{xy}. The applied magnetic field gives rise to a Lorentz force acting on the electrons, bending their paths towards the sample edge. (right) As electrons accumulate on one side of the Hall bar a transverse electric field, E_y, builds up. When E_y is sufficiently strong that it cancels out the Lorentz force due to the magnetic field, a steady state will be established in which the electrons maintain their average motion in the x-direction.*

$$R_H = \frac{V_H}{I} = \frac{B}{en_e}, \tag{1.1}$$

where n_e is the electron density per unit area in the xy-plane and e is the elementary charge. According to equation (1.1) the bigger the field, the stronger the Lorentz force and hence the bigger R_H will be. Furthermore, the lower the carrier density the greater the magnitude of R_H will be obtained. This follows from the fact that the lower the density the fewer electrons have to generate the same current and hence the faster the electrons will have to move. Electrons with bigger velocities (magnitude) experience stronger Lorentz forces and hence give rise to a bigger Hall voltage. Due to its simple form, and easy practical realization, the Hall resistance has become a standard tool for determining the carrier density of electrical conductors. In addition the Hall effect distinguishes between negatively and positively charged carriers.

1.2 The Quantum Hall Effect

A century after Edwin Hall found R_H to be linearly proportional to the strength of the magnetic field, Klaus von Klitzing and collaborators in 1980 found that in two dimensions this dependence looks much different[1]. Working in two dimensions and a regime of very low temperatures (below 4 K) and high magnetic fields ($1-10\,T$), they observed a stepwise dependence of R_H on magnetic field strength. These plateaus were accompanied by a simultaneous drop of the magneto resistance R_{xx} to zero, at sufficiently low temperatures [1]. Such observations indicate a dissipationless transport in the region of the plateaus - a so called *superflow*. What Von Klitzing and collaborators observed was the quantum Hall effect, an effect which is only observable in two dimensions, i.e. in two-dimensional electron systems.

1.2.1 Two-Dimensional Electron Systems

One might ask how such two-dimensional electron systems can be obtained in practice? There are several different ways:

One method is the MOSFET (metal-oxide-semiconductor field effect transistor). In a MOSFET the electrons are confined to the surface of a semiconductor, by sandwiching an oxide (insulator) in between the semiconductor and a gate. Applying and electric field through the gate, will put a drag on the conductance electrons of the semiconductor, pushing them against the impenetrable oxide-layer, hence creating a plane (two dimensions) of electrons[1, 2]. It was in a silicon MOSFET von Klitzing and collaborators discovered the quantum Hall effect[1, 3].

However, nowadays a more popular method for obtaining 2DES, used for quantum Hall measurements, is modulation doping. Modulation doping is obtained with molecular beam epitaxy (MBE), which allows for a highly controlled layer-by-layer growth of two different types of semiconductors, often GaAs and AlGaAs. It is important that the two semiconductors have almost identical lattice constants in order to minimize lattice imperfections, which will cause scattering of the electrons. The doping also introduces scattering in the form of the potential of the positively charged donors.

[1] For an explanation of this nontrivial lack of resistance at T=0, see section 1.2.4.

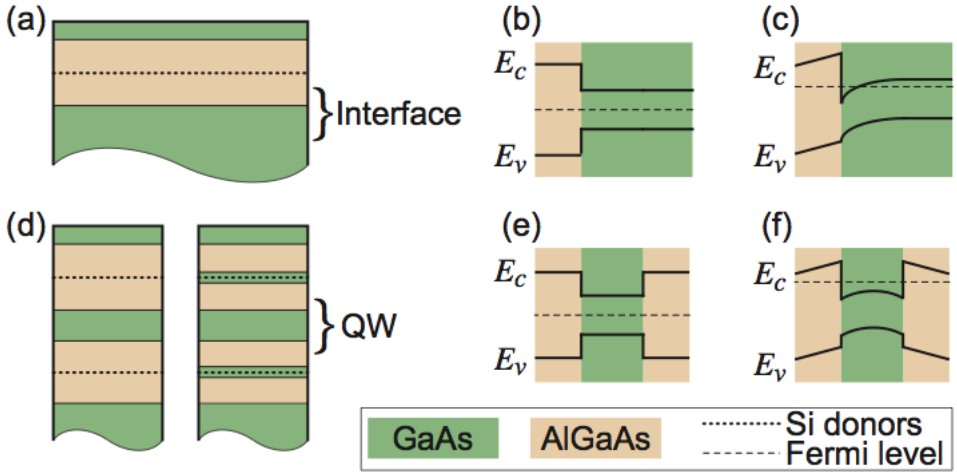

Figure 1.2: *Schematics of the layering and band structure in a GaAS/AlGaAs heterostructure (a-c) and a quantum well (d-f). (b) and (e) show the top of the valence band E_v and the bottom of the conductance band E_c before doping and (c) and (f) show the band gap structure after doping. The electrons are trapped in areas where $E_c < E_F$. Figure taken from [4].*

This scattering can be minimized by separating the electrons from their parent donors, confining them to a different plane of the material. In order to do so it is necessary for the two semiconductors to have a difference in band gaps, which exceeds the energy scale of the experiment. With the layered semiconductor structure one creates a "potential landscape" - formed by the conductance band energy- which will guide the doped electrons through the material, quantum mechanically binding them at the wished plane of the structure with help from either a quantum well or a heterostructure, see figure 1.2.

1.2.2 Quantization

Klaus von Klitzing and collaborators found the steps of R_H to be quantized in multiples of h/e^2[1]:

$$R_H = \frac{h}{\nu e^2}, \tag{1.2}$$

where h is Planck's constant, e is the elementary charge and ν is called the filling factor which is given by[5]

$$\nu = \frac{n_e}{B/\Phi_0}, \tag{1.3}$$

where $\Phi_0 = h/e$ is the quantum of flux. The filling factor is thus the ratio of electron density to the density of magnetic flux quanta, i.e. the number of electrons per unit flux piercing the sample. The plateaus can be understood within the context of Landau quantization.

Landau quantization

In strong magnetic fields electrons undergo cyclotron orbits, due the Lorentz force. The quantization of these cyclotron orbits is called Landau quantization. It restricts the charged particles

to orbits with discrete energy values - the so called Landau levels. The degeneracy is directly proportional to the magnetic field strength as described below.

In general the problem of electrons in a crystal, subject to a strong magnetic field cannot be solved exactly. An exact solution is only possible when the periodic lattice potential is ignored. As a reasonable approximation the problem can therefore be solved for a free electron gas confined to an area of sides L_x and L_y, with periodic boundary conditions.
The Hamiltonian, in the Landau gauge, for the unperturbed system (neglecting interaction terms) is,

$$H = \frac{p_x^2 + (p_y + eA)^2}{2m}, \;\; A = Bx\hat{y}. \tag{1.4}$$

From this it is seen that the system is translational invariant in the y direction. By rearranging the Hamiltonian it can be seen that the solution in the x direction is a linear harmonic oscillator shifted by[5],

$$x_0 = -\frac{\hbar k_y}{eB} = -\frac{\hbar k_y}{m_e \omega_c}, \;\; \omega_c = \frac{eB}{m_e}, \tag{1.5}$$

where ω_c is the *cyclotron frequency.*
The spatial translation of the potential does not change the energies so the energies (when neglecting spin) are given by the familiar Harmonic Oscillator energies:

$$E_j = \hbar\omega_c \left(j - \frac{1}{2}\right), j = 1, 2, 3... \tag{1.6}$$

Degeneracy of the Landau levels

From equation (1.6) it is seen that the energy does not depend on k_y. This leads to the degeneracy of the Landau levels. The number of possible states in a Landau level, i.e. the degree of degeneracy is given by the possible values of k_y. When periodic boundaries are assumed, the quantization of the k_y quantum number is given by,

$$k_y = \frac{2\pi N}{L_y}, \tag{1.7}$$

where N is an integer. In addition, the requirement that the center of the oscillator lies within the system $0 \leq x_0 < L_x$ must be fulfilled. When joined with equation (1.5) this constraint implies that k_y must be within the range

$$-\frac{m_e \omega_c}{\hbar} L_x \leq k_y < 0. \tag{1.8}$$

From this it can be shown that the number of allowed values for k_y is given by

$$N_{max} = \frac{eBL_xL_y}{h} = \frac{\Phi}{\Phi_0}, \tag{1.9}$$

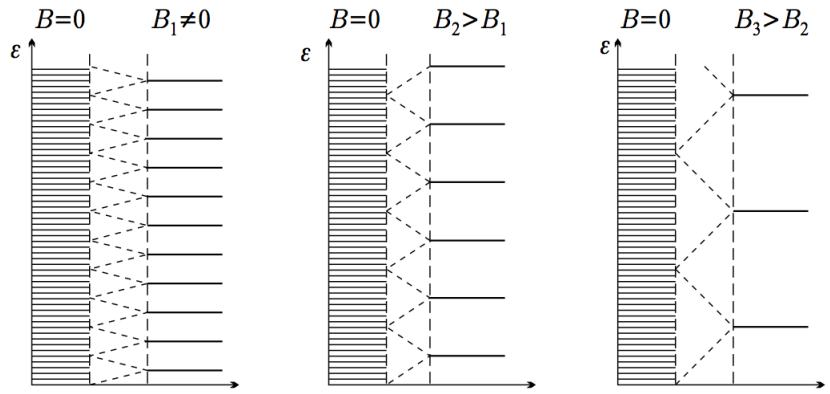

Figure 1.3: *As the magnetic field increases, more and more electron-states "condense" into each Landau level. Simultaneously the distance between adjacent Landau levels increases. Figure taken from [5].*

where $\Phi = BL_yL_x$ is the total magnetic flux through the system. The value of N_{max} depends linearly on B, so the degeneracy of the Landau levels increases with increasing magnetic field. As B is increased more and more states "condense" into Landau levels of lower quantum number, j, whilst the distance $\hbar\omega_c$ between adjacent levels increases. It should be noted that the degeneracy is a general property of each Landau level, in principle independent of material properties.[2]

The effects of Landau quantization are only observed when the thermal energy is smaller than the separation energy of the landau levels, i.e. when $k_{\mathrm{B}}T \ll \hbar\omega_{\mathrm{c}}$. Put in other words

> *The Landau quantization is only observed for low temperatures and large magnetic fields.*

If the spins of the electrons are taken into account, there will be Zeeman splitting of the Landau levels, due to the extra energy term $\pm\frac{1}{2}g_e\mu_B B$, where μ_B is the Bohr factor and g_e is the electron spin g-factor.

1.2.3 Filling Factor

The filling factor is, as the name suggests, the number of filled Landau levels, i.e. ν is equal to j for the top most filled Landau level.
In the simple picture given above, the electrons exactly fill up an integer number of Landau levels, at specific magnetic field values:

$$B_\nu = \frac{n_e h/e}{\nu} = \frac{n_e \Phi_0}{\nu}, \tag{1.10}$$

leaving all higher levels empty. Filled Landau levels are incompressible meaning that, exciting an electron from the Landau level has a nonzero energy cost[6]. This is essential for the explanation of why R_{xx} drops to zero at filled Landau levels.

[2]Some materials have multiple valleys in the conductance band, hereby increasing the degeneracy.

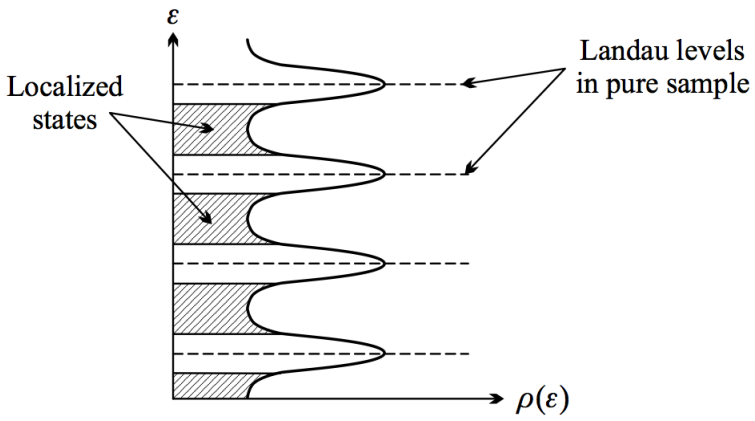

Figure 1.4: *The degenerate Landau levels of an ideal 2DEG are illustrated by dashed lines (the density of states given by Dirac delta functions). In a real (imperfect) 2DEG these states broaden into bands, with extended states near the ideal Landau level (white boarders), separated by localized states (shaded). Because the localized electrons do not contribute to the transport, one can say that there is a "mobility gap". Figure taken from [5].*

Consider starting at magnetic field $B_1 = n_e h/e$, where all electrons fit into the first Landau level. Decreasing the field strength will decrease the capacity of the first Landau level, cf. equation (1.9), hereby forcing electrons to occupy states in the next higher Landau level. According to this picture R_H would take on quantized values only at very precise values[3] of the magnetic field, as given in equation (1.10). This would result in measurements showing the same linear dependence of R_H on B as for the classical Hall effect.
In the above discussion of Landau quantization, one very important assumption was made: the electrons constitute a two-dimensional *free* electron gas. More realistically we should also consider localization of electrons due to impurities and imperfections in the lattice. Such perturbations create potential valleys where electrons can be trapped and isolated, hence excluding them from the electrical conduction, see figure 1.4. For a finite change in magnetic field, all changes in degeneracy happens within the localized state and because they do not take part in the transport, this leads to a stretching of the given plateau in R_H and associated drop in R_{xx}. This broadening of the plateaus enables us to detect the quantum Hall effect.

Note that, if the motion were not restricted to two dimensions, the extra energy term, $\hbar^2 k_z^2/2m_e$, would fill the mobility gaps with a continuum[4] of available states. Thereby eliminating the quantum Hall effect.

1.2.4 Edge States

In the semi-classical picture, in the absence of any electrical field, electrons in a magnetic field move in circular orbits with the cyclotron radius, $r_c = (2m_e\epsilon)^{1/2}/eB$, in the plane perpendicular to the B-field[5]. This picture is only applicable in the bulk of the sample where the potential is approximately constant. Near the edges of the sample, where the oscillator's coordinate x_0 is less

[3] With a sample size of $1mm^2$, the field value needed to move away from a plateau is $4 \cdot 10^{-21}$ T, corresponding to one flux quantum.
[4] Strictly speaking, one would assume periodic boundary conditions in the z direction, which would quantize k_z. The energy separation is however so small that it can be regarded as a continuum.

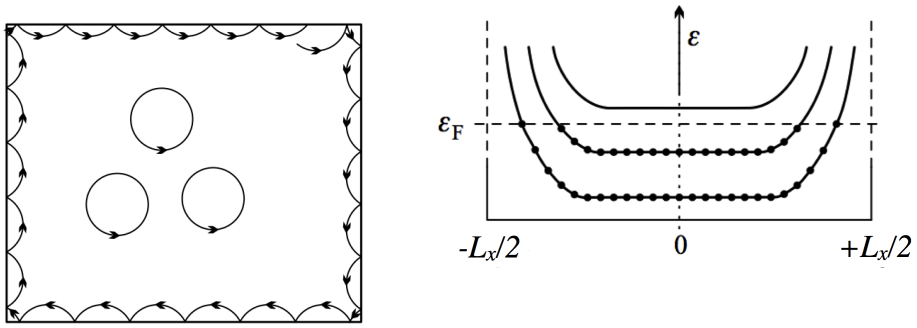

Figure 1.5: *(left) Electrons traversing circular arcs along the edges of the sample, leading to a current flowing in one direction along the edge of the sample. In the bulk of the sample no current runs, since there is no electron transport, i.e. the electrons circle around their orbit midpoints.*
(right) Bending of the Landau levels near the edges of the sample gives rise to compressible strips (1-dimensional conducting wires) occurring at the intersection of the Landau levels with the Fermi level. The dots represent occupied states. Figures taken from [5], right figure has been modified.

than r_c from the edge, the electrons are repeatedly reflected back from the potential wall, resulting in a "skipping" trajectory of circular arcs along the edges, forced by the magnetic field to go in only one direction around the sample edge, see figure 1.5[5].

In a quantum mechanical approach this motion along the edge can be pictured as an upwards bending of the Landau levels near the edges of the sample, due to the confining potential as illustrated in figure 1.5. The direction of motion along the edges is given by the slope of the bended level, i.e. $V_{g_y} = \frac{\partial \epsilon}{\partial k_y}$, where the level intersects the Fermi level.

In a filled Landau level, there is no freedom for scattering of the edge states (due to the incompressibility of filled Landau levels - there simply are no vacant states, of less or equal energy, which the electron can be elastically scattered into), and therefore there will be no variation in the chemical potential measured along one side of the sample (longitudinal measurement), i.e. there will be no resistance. This is the explanation of R_{xx} dropping to zero at the exact filling of Landau levels[6].

1.2.5 Fractional Quantum Hall Effect

The phenomenon described above is called the integer quantum Hall effect, abbreviated IQHE, because it occurs for integer values of the filling factor. But when going to magnetic fields higher than $B_1 = n_e h/e$, where the first Landau level is only partially filled, one will see new plateaus emerging at values of magnetic field corresponding to fractional filling factors. This is the so called fractional quantum Hall effect which was discovered in 1981 by Horst L. Störmer, Dan Tsui and Art Gossard[1]. Störmer et al. observed a plateau at a $R_H = h/\nu e^2 = 3h/e^2$, indicating a filling factor of $\nu = 1/3$. From equation (1.3) it is seen that the filling factor is the ratio of electrons to flux quanta, $\nu = p/q$. Hence what Störmer and collaborators observed was a situation of three flux quanta per electron.
The IQHE can be described as a single particle effect, as all interactions between the electrons

[5]For magnetic fields pointing out of the plane of the sample, the edge states move clockwise and for magnetic fields pointing into the plane of the sample they move anticlockwise.

are neglected and the role of other electrons primarily is to fill up the empty states of the Landau levels. In contrast the fractional quantum Hall effect follows from electron-electron interactions. This renders it to be an intrinsically many-particle effect. In general, many-particle effects are challenging to deal with theoretically. In some cases they can be treated as minor corrections (perturbations) to a known problem and can therefore be solved with perturbation theory, using the eigenstates of the known system. For the FQHE, however, this is not the case. The electron-electron interaction is the essence of the FQHE, and this interaction modifies the ground state so much that it can no longer be regarded as a perturbation. To solve the FQHE problem one had to construct a completely new class of wave functions.

Composite particles and quasi particles

In 1998 Bob Laughlin won the Nobel prize (together with Tsui and Störmer) for his contribution to the formalism of FQHE, which he published in 1983. Laughlin presented a many-particle ground state wave function which allowed for a description of all FQHE states of filling factor $\nu = 1/q$, where q is bound to be an odd integer in order to ensure antisymmetry[6, 3]. Due to the Laughling-Jastrow factor, $(z_j - z_k)$, nodes are created in the Laughlin wave function, whenever the positions of two electrons, z_j and z_k[6] coincide[3]. In this way the spatial correlations between the electrons, i.e. the electrons minimizing their Coulomb energy, are taken account for. According to the Laughlin wave function, a free electron moving on a closed path around a node (a fellow electron kept fixed) will obtain a phase, $\theta = 2\pi/\nu = q2\pi$. Since the Aharonov-Bohm phase acquired by an electron, moving on a closed path around q flux quanta, is also given by $q2\pi$, one can picture this as a coupling of q flux quanta to each electron[3]. The coupling of flux quanta and electrons is interpreted as a new kind of particles, so called composite particles (CP's). The CP's interact differently than the bare electrons since all of the magnetic field is now incorporated in the particles, hence leading the CP's to sense no magnetic field. When detuning the magnetic field from the value for exact filling of a level, an excess of either flux quanta or electrons will arise. The amount of charge respectively deficit or surplus amounts to $e^* = \pm e/q$, hence leading to quasiholes (excess flux quanta) and quasielectrons (excess electrons) of fractional charge. These *qausiparticles* play the role of charge carriers in the FQHE.

As more fractions were discovered, many of which did not fit into the Laughlin theory, which only took account of the fractions $\nu = 1/q$ and their particle-hole symmetric counterparts $\nu = 1 - 1/q$, a need for a more comprehensive explanation emerged.

The composite fermion model and filling factor 1/2

As an generalization of Laughlin's theory, Jainendra K. Jain proposed the *composite fermion theory*, in which a composite fermion is a bound state of an electron and an even number, *2p*, of quantized vortices. Coupling an even number of flux quanta with each electron leads to Fermi-Dirac statistics, since exchanging two bare electrons in space introduces a factor of -1 to the wave function and in addition to this each 'attached' flux quanta will introduce another factor of -1. The strongly interacting electrons hereby turn into weakly interacting composite fermions, hence making it possible to explain the FQHE as an IQHE of composite fermions, with integer effective filling factors, ν^*. The composite fermions having an effective filling factor $\nu*$ corresponds to a

[6]The electron coordinate z_j is a complex number, $z_j = x_j + iy_j$

ν^*	ν
1	1/3
-1	1
2	2/5
-2	2/3
3	3/7
-3	3/5

Table 1.1: *Negative values of ν^* corresponds to negative values of the effective field B^*.*

situation in which they experience an effective magnetic field B^*, different from the actual field B. The relation between the fractional filling factor and the effective integer filling factor is given by[6]:

$$\nu = \frac{\nu^*}{2p\nu^* \pm 1}, \tag{1.11}$$

where the sign in the denominator is due to respectively a positive and a negative value of B^*.

The motivation for such a model is in great part given by the absence of a plateau at $R_H = 2h/e^2$, concomitant with the observation that R_{xx} symmetrically performs Shubnikov-de Haas-like oscillations around $\nu = 1/2$. This suggest that the FQHE is just the integer IQHE of a new kind of particles feeling zero magnetic field at $\nu = 1/2$. As the attentive reader might have noticed $\nu = 1/2$ is itself not contained in the sequence of equation (1.11), but is obtained as $\nu^* \to \infty$. If the model of noninteracting CF's remains valid in this limit, the observation described above can be explained as the coupling of two flux quanta to each electron, whereby all of the magnetic field is incorporated in the CF's, leading to a situation of no exerted magnetic field, i.e. a Fermi sea of CF's. Moving on to $\nu = 1/3$ one extra flux quantum is introduced per CF. Since the CF-model does not allow for these flux quanta to couple to the CF's, this gives rise to an effective magnetic field corresponding to that of $\nu = 1$ in the IQHE of electrons, i.e. $\nu = 1/3 \longrightarrow \nu* = 1$. The CF's feel the effective magnetic field[6]:

$$B^* = B - 2pn_e\phi_0 \tag{1.12}$$

The sequence described by equation (1.11) does not cover all the fractions observed, but other sequences exist within the CF-model, whereby almost all fractions are covered[7]. In the CF-model the understanding of quasiparticles and quasiholes is equivalent to that of the Laughlin states, i.e. they arise from an excess or deficit of flux quanta. A CF-exciton is an excitation of a CF from one CF-level to a higher, effectively creating a quasiparticle-hole pair.

Even though it is convenient with mental pictures such as flux quanta and flux attachment one should always keep in mind that they are simplifications of reality and should not be taken too literally. The magnetic field is itself not quantized but uniformly spread over the whole sample.

[7]Only excluding even denominator fractions and some few odd denominator fractions.

Filling factor 5/2

One of the fractions not covered by the sequences of the CF-model is $\nu = 5/2$. Zeeman splitting of the Landau levels leads to spin polarized levels, i.e. each IQHE-level consist of two spin polarized sub-levels. Writing $5/2$ as $2 + \frac{1}{2}$, and counting the first Landau level as two levels, due to the Zeeman splitting, one can regard $\nu = 5/2$ as a half filled second Landau level. Hence it is widely believed that $\nu = 5/2$ is a spin up polarized level. Normally one would expect $\nu = 5/2$ to behave like $\nu = 1/2$ and $\nu = 3/2$, which do not have any energy gaps and therefore can be described in terms of a Fermi sea. This is clearly not the case for $\nu = 5/2$, where a well defined FQH-plateau is observed, indicating the presence of an energy gap. Within the CF-model the CF's can lower their energy by pairing up in a p-wave like pairing[6], hereby creating the energy gap necessary.

Starting out in the IQHE-regime, electron-electron interactions can be neglected, but as magnetic field strength is increased, hence moving to the FQHE-regime, these interactions can no longer be neglected. Introducing the formation of composite particles, one can again neglect the interaction. At $\nu = 5/2$ the interaction between the CF's can no longer be ignored, but as the CF's pair up, forming bosons, a state of weakly interaction particles will again arise.

The explanation of FQHE provided here, is very brief and simplified. A great deal of further theories and additions has been proposed. For a more detailed understanding of the FQHE we refer to [6] and [1].

Chapter 2

Setup

The experimental setup used to measure IQHE and FQHE requires as a minimum, a cooling source that can cool to approximately 20 mK, a magnet which must be able to produces steady fields up to at least 10 T, low noise lock-in amplifiers and a good way of electrically measuring the sample without introducing to much heat and noise. This chapter describes the different techniques used to fulfil these requirements.

2.1 Cryofree Dilution Refrigerator

The IQHE and especially the FQHE can only be observed if the electron temperature is sufficiently low. To cool electrons below 25 mK, we use a cryofree dilution refrigerator (fridge) from Oxford Instruments, which is capable of producing stable temperatures as low as 10 mK, see figure 2.1. The fridge produces these low temperatures by circulating ^{3}He through multiple heat exchangers and at the final stage, called the mixing chamber, by mixing rich ^{3}He with superfluid ^{4}He.
Cryofree dilution refrigerators, also called dry fridges, are a fairly new invention, previously the dilution fridges were wet. Wet means that they use liquid nitrogen and helium to cool the ^{3}He on it's way down, instead of a pulse tube cooler. The wet fridge is believed to be less noisy than its dry cousin because it does not need a pulse tube cooler and therefore it would be more suited for FQHE measurements. So why would one choose a dry over a wet fridge? There are two main reasons: Dry fridges do not consume a lot of expensive helium and nitrogen during operation and more importantly, they have less down time due to malfunctions. We show that, with sufficient heat sinking, it is possible to measure very sensitive FQH states with a running pulse tube cooler on a dry fridge, see chapter 3.
The fridge cools in two stages, a pre-cool stage and a condensing stage, see figure 2.1. The pre-cool stage is powered by a two-stage pulse tube cooler that cools the mixture at the two top most plates (PT1, PT2) via heat exchangers, which then cools the still, 100 mK and mixing chamber plates, by similar heat exchangers at the lower plates. The pre-cool stage can cool the mixing chamber plate to approximately 4 K, but normally condensing is initiated just below 10 K.
It is the condensing stage that makes the fridge reach very low temperatures. The trick is to condense the ^{3}He gas to liquid, which then can be mixed with superfluid ^{4}He in the mixing chamber and by that process cool the mixing chamber plate to 20 mK or lower. The pulse tube cooler is a vital part of the condensing stage as it cools the ^{3}He below its inversion temperature[8], allowing a Joule-Thomson (trotteling) process to isenthalpic expand the gas[9]. This expansion

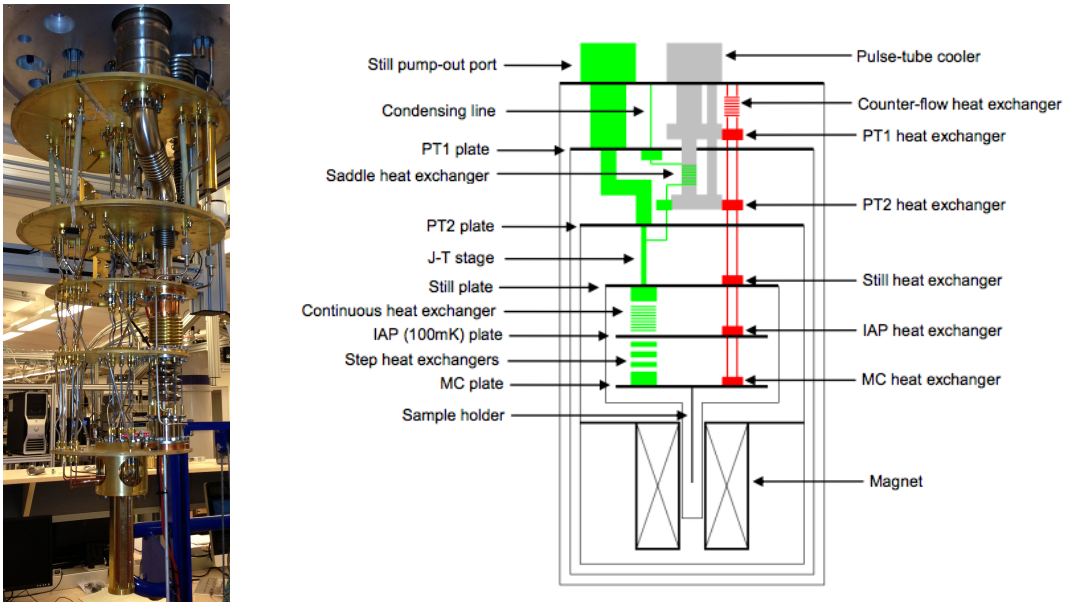

Figure 2.1: *The fridge, without vacuum cans (left). The right picture shows an overview of the cooling stages, condensing (green) and pre-cool (red), figure taken from [7].*

cools the ^{3}He even further which allows it to condense. The condensed ^{3}He is then mixed with ^{4}He in the mixing chamber, where it will separate into two phases. One phase which is almost pure ^{3}He and another (diluted) phase containing ^{4}He mixed with approximately 6% ^{3}He, see figure 2.2. The diluted phase is connected to the still chamber where ^{3}He is selectively removed by a weak heater and low pressure. This selective removal allows for continuous operation of the cooling cycle. The low pressure is produced by a turbo pump mounted on top of the fridge. To restore equilibrium in the mixing chamber ^{3}He has to jump through the phase boundary, this process costs energy which is taken from the mixing chamber plate[10].

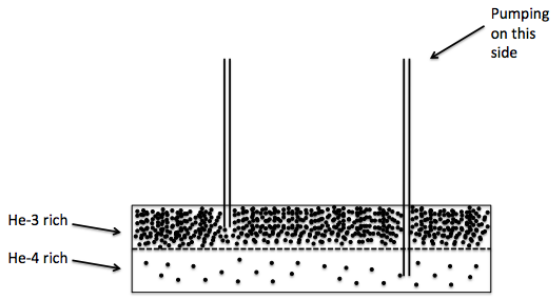

Figure 2.2: *Diluton process in the mixing chamber, on the top is the* ^{3}He *rich phase and in the bottom is the diluted phase.*

2.2 Heat Sinks

In order to electrically measure the sample you need wiring that runs from the sample to room temperature. This can potentially introduce a big heat load on the sample, because the wires apart from being good electrical conductors also are excellent thermal conductors. This is true

because lattice vibrations (phonons) are almost absent in the mK range and therefore the Wiedemann–Franz law can be used. The Wiedemann–Franz law states that the ratio between the thermal conductivity (κ) and the electrical conductivity (σ) is proportional to the temperature. Therefore κ is proportional to σ[5]. Because of this, it is crucial to minimize the thermal link to room temperature as much as possible. To do that we have installed several different heat sinking components in the fridge.

Clamps On the first two plates (PT1 and PT2) a clamp is installed, which insures a good thermal link between wires and plates. At this point there are no need for further heat sinking, because of the relatively high temperature. The clamps will introduce a heat load to the plates, but because of the pulse tube cooler's large cooling power, the heat is easily removed again. At these plates the dominant heat load is generated by other heat sources, e.g. coax lines.

Bobbins Heat sinking on the still and 100 mK plates is facilitated by bobbins, see figure 2.3. Bobbins are copper posts where the wires are wrapped around and fastened to give a good thermal contact. The main difference between clamps and bobbins is the length of wire that can be thermalized and because of that bobbins are desirable at these low temperature plates. It will introduce a relatively big heat load at the lower plates (100 mK and mixing chamber) if the wires are not properly thermalized on the still plate.

Sapphire boxes and signal filters On the mixing chamber plate we have installed three sapphire boxes and two signal filters. The sapphire boxes are composed of a sapphire substrate, with UV lithographic patterned gold meanders, mounted on a gold plated PCB, see figure 2.4. The PCB is then clamped between gold plated high conductivity copper brackets, see figure 2.3. We have chosen sapphire because it possesses two important properties: It is an insulator and at the same time it has a relatively high thermal conductivity at low temperatures. The sapphire boxes yield a good thermal link to the mixing chamber plate by a fairly long and resistive path through the gold meanders. The resistance through each meander line is approximately 1 kΩ, which together with the 200 Ω and two 1 nF capacitors in the RC filter gives a low pass cut off frequency of roughly 5.5 kHz. Not all lines in the RC filter have these small capacitors, some have two 200 nF capacitors instead. These are used to power gates, which need heavy filtering to get rid of all non DC noise. The last signal filter is a band pass filter with a range from DC to 80 MHz. It's made from three different surface mounted filters that combined gives the DC to 80 MHz range. Both the RC (low pass) and the RF (band pass) filter are mounted on the mixing chamber plate with gold plated high conductivity copper brackets.

2.3 Eddy Currents

According to Faraday's law of induction, a change in magnetic flux will induce an emf.

$$\mathcal{E} = -\frac{d\Phi_B}{dt} \tag{2.1}$$

This emf will give rise to a current in any closed conducting loop. This current is called Eddy current and the power dissipated in a perpendicular plane loop will be $\mathcal{E}^2/R$ where R is the

Figure 2.3: *The left photo shows a bobbin installed on the bottom of the still plate. The right shows sapphire heat sinks and signal filters mounted on the mixing chamber plate.*

resistance in the loop[4]. This also means that low resistance metal will give rise to a larger power dissipation, so building a fridge with large cross sections of copper or silver, near the magnet, would be inexpedient in respect to Eddy currents, but profitable in respect to thermalization. To prevent large eddy currents slots are cut in the plates. These cuts reduces the effective area and thereby the induced Eddy currents.
Because the FQHE is very temperature dependent the rate in which the magnet is swept is very important, we have found that a sweep rate above 20 mT/min induces more heat per unit time than the fridge can cool.

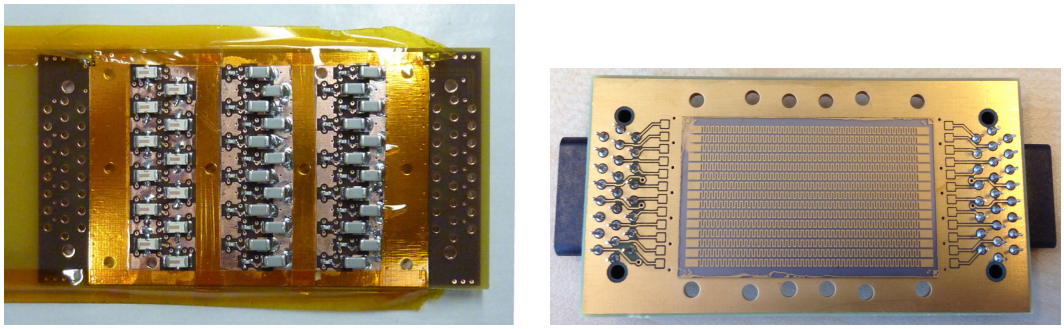

Figure 2.4: *The photos shows a RC-filter (left) and a sapphire heat sink on the PCB (right).*

2.4 Puck

A puck is a hollow cylinder made from brass that can hold a sample holder. It connects electrically and thermally to the coldfinger beneath the mixing chamber plate. The electrical connection is facilitated by a 51 pin nanoD connector. The puck can also connect to a Load Lock through two nanoD connectors. The puck accepts 14 smp connections, hereby connecting the coax lines to the sample.
Together with a Load Lock, the puck can enable fast sample changes, without warming the fridge to room temperature and taking all the vacuum cans off. This process normally requires 2 days and an additional 2 days to cool down again. With the new system a sample change and cool down can be done in a few hours. Quantum Hall measurements require perpendicular magnet fields, which meant that we had to design a sample holder with appropriate orientation. To insure good thermalization the mount is cut out of a single piece of high purity copper, see figure 2.5, and mounted to the top plate of the puck.

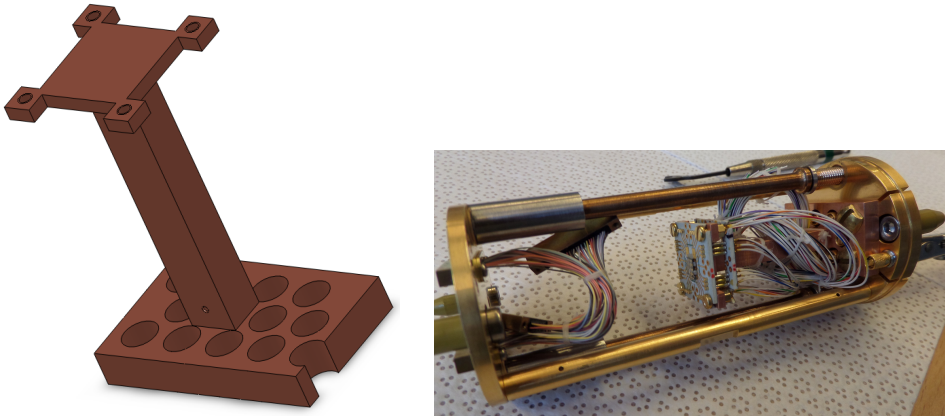

Figure 2.5: *The copper mount, mounted inside a puck (right) and a solidworks model of the copper mount (left). See Appendix D for the solidworks design file.*

2.5 Wiring

There are two types of signal lines in the fridge, high and low frequency lines. The high frequency signals are transported in 16, 50Ω coax lines that run from the top of the fridge to the mixing chamber, with 14 lines running to the coldfinger. We do not use the high frequency lines in our experiments, so to prevent them from radiating heat to the sample all coax lines are terminated with a 50Ω shorting cap inside the puck. The shorting cap converts any signal to heat. which is then removed from the puck by the coldfinger.
The fridges in QDev all normally have 48 low frequency lines in each fridge, but our (Triton 2) has only 24. All 24 lines are woven into a "carpet" called loom and twisted pairwise into 12 pairs, see figure 2.6. We use two different materials as conductors, constantan and copper[1]. The constantan loom is used from room temperature to the mixing chamber plate. Constantan has a much higher resistivity than copper, but is not temperature dependent, which makes it perfect for transporting signals from 10 mK to room temperature. At the mixing chamber and below, we can use copper loom in order to provide as much cooling power as possible to the sample holder.

[1]Copper loom part no: A8-312, Constantan loom part no: A8-311

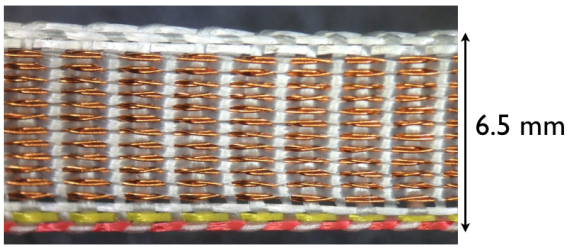

Figure 2.6: *A piece of copper loom*

2.6 Noise Reduction

To get a clean signal, it is essential to reduce the noise in the experimental setup. The noise in the signal can be removed by raising the integration time of the lock-in amplifiers. Doing so will mean an increase in acquisition time, if the same signal to noise ratio has to be archived. Therefore it is crucial to reduced the noise in the measurement setup.
Especially 50 Hz noise can be a big source of noise if different groundings are used. There are generally three things to be extra aware of when setting up a measurement station:

- Keep all instruments on the same ground as the fridge.
- When using BNC cables, don't use the shield as a signal conductor[11].
- When connecting instruments to the fridge via BNC cables, try to avoid adding an additional ground to the first instrument that receives the signal from the fridge, in our case two pre-amplifiers[11].

Whenever a new instrument is incorporated into the setup, one should always think about ground loops. Ground loops arise when two connected circuits are both grounded with different grounds, there can even be potential fluctuations on the same ground if the connection is not made at the physically same point, see figure 2.7. Another noise source associated with ground loops are induced currents due to changing the magnetic field.

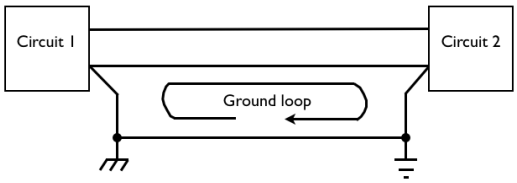

Figure 2.7: *A ground loop will be induced if circuit 1 and circuit 2 is connected to different ground potentials, or if there is a changing flux through the loop.*

2.7 Data Acquisition

The instruments used in our setup can be divided into two categories: Control and acquisition. On the control side we have the magnet power supply and the gas handling unit, see figure 2.8. The magnet power supply can be controlled from matlab, which allows fast readouts and programmable

automation of sweeps. The gas handling unit controls everything else in and around the fridge, i.e. the circulation of mixture, pumps and heaters. The gas handling unit has a dedicated computer which can be accessed through Ethernet to read out cooling water and fridge temperatures. The

Figure 2.8: *The magnet power supply (left) and the gas handling unit (right).*

instruments used to acquire data are: Stanford Research SR830 Lock-in amplifiers, NF Electronic Instruments LI-75A pre-amplifiers and a DecaDac built by Jim MacArthur at Harvard University. The pre-amplifiers are used between the fridge and the SR830's to minimize noise, because they have a very low input referenced noise level. The DecaDac is used for biasing potential gates. The lock-in amplifiers are used to ensure filtering of noise in the signal. The lock-in amplifiers operates by looking for a specific frequency in the signal, that of course have to be the same frequency as the biasing signal. This "looking" is done by a multiplication of the incoming signal with the reference signal (output)[12]. If the reference signal is $V_r sin\left(\omega_r t + \theta_r\right)$ and the measured signal is $V_m sin\left(\omega_m t + \theta_m\right)$ then

$$\begin{aligned} V &= V_r V_m sin\left(\omega_r t + \theta_r\right) sin\left(\omega_m t + \theta_m\right) \Rightarrow \\ V &= \frac{1}{2} V_r V_m cos\left(\left(\omega_m - \omega_r\right) t + \theta_m - \theta_r\right) - \frac{1}{2} V_r V_m cos\left(\left(\omega_m + \omega_r\right) t + \theta_m + \theta_r\right) \end{aligned} \tag{2.2}$$

is the multipled signal.
The multiplied signal is now low pass filtered and all the AC components are removed, which means that the feed through will be zero unless $\omega_m = \omega_r$. This will make the first half of equation (2.2) a DC signal which will pass through the low pass filter. The signal passed through is therefore phase sensitive:

$$V = \frac{1}{2} V_r V_m cos\left(\theta_m - \theta_r\right).$$

Internally, the lock-in has two reference signals to avoid a total loss of signal, if the measured signal is totally out of phase (90°). The second reference signal is $V_r sin\left(\omega_r t + \theta_r + \frac{\pi}{2}\right)$ which then makes

the lock-in capable of measuring the out of phase signal. The two measured signals are called X and Y and they are

$$X = V_m cos\left(\theta_m - \theta_r\right)$$
$$Y = V_m sin\left(\theta_m - \theta_r\right).$$

The total magnitude is called R and the angle between X and Y is called θ, they are,

$$R = \left(X^2 + Y^2\right)^{1/2} \Rightarrow$$
$$R = V_m$$

$$\theta = arctan\left(\frac{Y}{X}\right) \Rightarrow$$
$$\theta = \theta_m - \theta_r.$$

X,Y,θ and R are produced numerically by the SR830.

2.8 Wafer

For our measurements we have used the sample WC2-P2-22-10.1, which is a square mesa chip. This notation is of the form XYN-ZM-DD-YY.N, where XY are the initials of the person who cleaved the chip (in this case Willy Chang), Z is the name of the grower (in this case Pfeiffer), M-DD-YY is the month, day and year and N is a serial number. Most square mesa chips contain sixteen mesas, each containing one device or none, arranged in four rows (A through D from top to bottom) and four columns (1 through 4 from left to right), with an orientation such that alignment marks are located at the bottom of the chip. Our measurements were performed on mesa C2, which

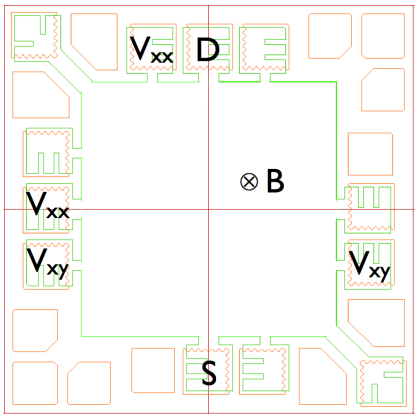

Figure 2.9: *Design cad drawing of the mesa used for our measurements. The green lines indicate the edge of the 2DEG. We have performed six-terminal measurements. Ohmics S and D are used as source and drain*

is just a bare mesa with no device on it, see figure 2.9. The data presented in the next section is taken as six-terminal measurements. Since in the QHE the current flows along the edges, the way to distinguish a Hall-measurement from a longitudinal measurement is in principal given by the topological sequence of ohmics used for measuring voltages and applying current. A longitudinal

measurement is given by the topological sequence IIVV, and a Hall-measurement by the sequence IVIV. In general you would want to measure the longitudinal voltage drop over a distance as large as possible in order to get a bigger signal.
Our device is fabricated on a GaAs/AlGaAs wafer containing a 40 nm wide quantum well located approximately 275 nm below the surface of the wafer, see figure B.1. The 2DEG has a mobility of $\mu = 19 \cdot 10^6\ cm^2/Vs$ and a density of $n = 1.6 \cdot 10^{11}\ 1/cm^2$.

Chapter 3

Data

3.1 QHE in a GaAs/AlGaAs QW structure

Figure 3.1 shows a measurement of R_{xx}, longitudinal resistance (red), and R_{xy}, Hall resistance (blue), as a function of B. The plot displays countable integer steps from $\nu = 1$ to $\nu = 16$ and fractional plateaus between $\nu = 1$ and $\nu = 2$ and between $\nu = 2$ and $\nu = 3$. The measurement was done with a current bias $I_b = 4$ nA and at lock-in frequency $f = 111$ Hz. The magnetic field was swept from 7 T to 0 T with a rate of 3 mT/min, with the field pointing into the face of the mesa, see figure 2.9.
Figure 3.2 shows a sweep from 12 T to 7 T, with clear plateaus at $\nu = 1, 4/5, 5/7, 2/3$. The bias current used in this sweep was $I_b = 6$ nA at a lock-in frequency $f = 63$ Hz. The sweep rate was 5 mT/min. Until ~ 1.7 T we see only integer plateaus in the Hall resistance and Shubnikov-de Hass oscillations in the longitudinal resistance. We don't see any fractions until $\nu = 5/2$ at 2.9 T. We would have liked to see $\nu = 7/2$, but it didn't show, presumably because the temperature isn't low enough. Around 5 T we see a similar effect of what other people have seen around $\nu = 1/2$[1], which corresponds to formation of composite fermions in zero magnetic field in the lowest spinfull Landau level. The effect we see at $\nu = 3/2$ shows the same behaviour as $\nu = 1/2$ and can also be explained within the CF model as the formation of composite fermions in zero magnetic field in the second spinfull Landau level, see figure 3.1. The difference between the two CF states is the orientation of the spin, $\nu = 1/2$ has spin up and $\nu = 3/2$ has spin down. The states around $\nu = 3/2$ can be described as an IQHE for CF's with the formula[6]

$$\nu = 1 + \frac{\nu^*}{2\nu^* \pm 1}$$

The same effect is seen around 10 T, this is $\nu = 3/4$, see figure 3.2.

The integer plateaus have been found to agree so well with the exact quantization values of $R_H = \frac{1}{\nu}\frac{h}{e^2}$ that any deviation from the exact value is regarded as some measurement induced offset, that has to be corrected. Our data shows deviations from the exact quantized values, as seen in figure 3.1 and figure 3.2. The offset is especially large at high magnetic field, $\nu = 2/3$ at 11 T is closer to $1.45h/e^2$ than to $1.5h/e^2$ which is the correct value. To correct for this offset, we have tried two different methods. One of which was making a resistor model where the total line resistance and the gain of the pre-amplifiers was corrected, by fixing two plateaus to the exact

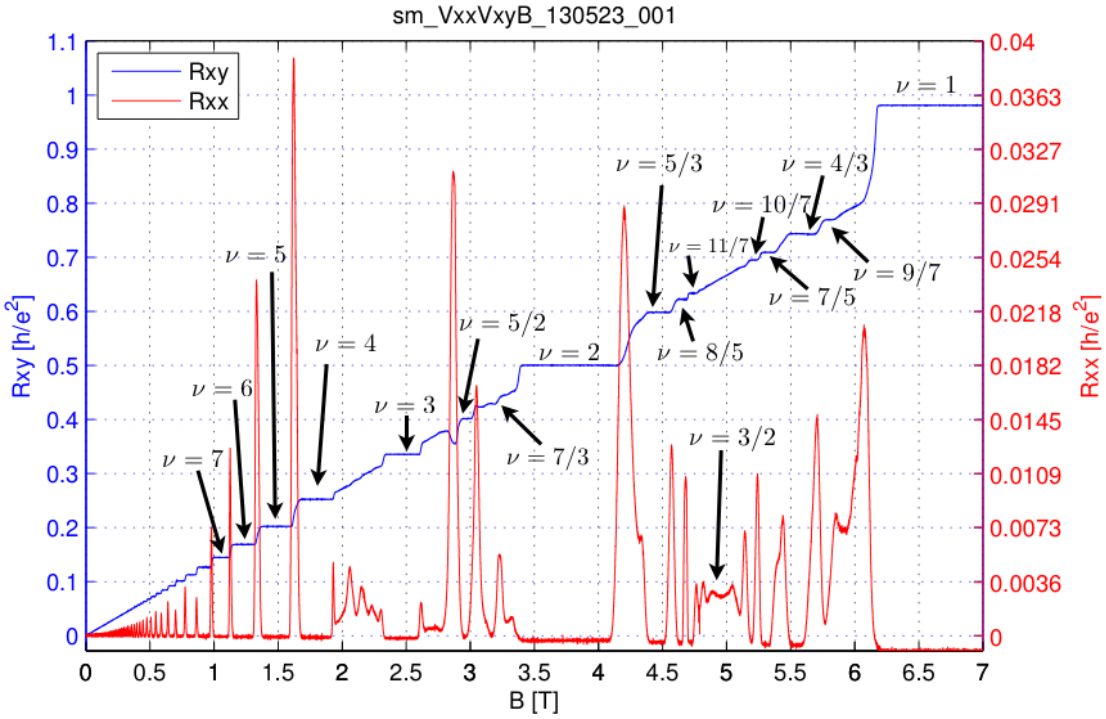

Figure 3.1: *Hall (blue) resistance and longitudinal (red) resistance as a function of magnetic field at ∼ 20 mK. The Hall trace shows regular integer plateaus and Shubnikov-de Haas oscillations until ∼ 2 T. After 2.5 T there are a lot of fractions, in particular $\nu = 5/2$ which occurs at 2.9 T. Data from mesa C2 on WC2-P2-22-10.1*

quantized value. The other method we tried was correcting the data with a linear model (y = ax +b) also by fixing two plateaus. Non of the two methods gave a good correction. The resistor model predicted a line resistance 200 $k\Omega$ below our bias resistor, which lead to an overshoot of the plateaus. The best linear correction we obtained corrected the higher plateaus but made the lower plateaus worse. On top of that the R_{xy} resistance became negative at zero magnetic field.
Our best explanation of this effect is that the assumption of constant current, with a 1 $M\Omega$ bias resistor, was not correct. Using a bigger bias resistor or measuring the voltage drop over the bias resistor might give the correct values.

The regions of zero R_{xx} have an overall negative slope, which means that the resistance becomes negative as the field is increased. We believe that this effect is an artifact of the capacitors in the low pass filter. The R_{xx} value at 7 T is more negative in the low field plot, figure 3.1, than in the high field region, figure 3.2. This can be explained by the fact that the high field data was taken with a lower frequency. To check our hypothesise about the frequency dependence of R_{xx}, we measured R_{xy} and R_{xx} using lines with two 200 nF capacitors, instead of two 1 nF capacitors. The result can be seen in Appendix C.

3.2 2DEG temperature

The temperature of the 2DEG is in general not the same as the mixing chamber. It can be higher and lower. A good way to tell your 2DEG temperature is by looking at some of the most

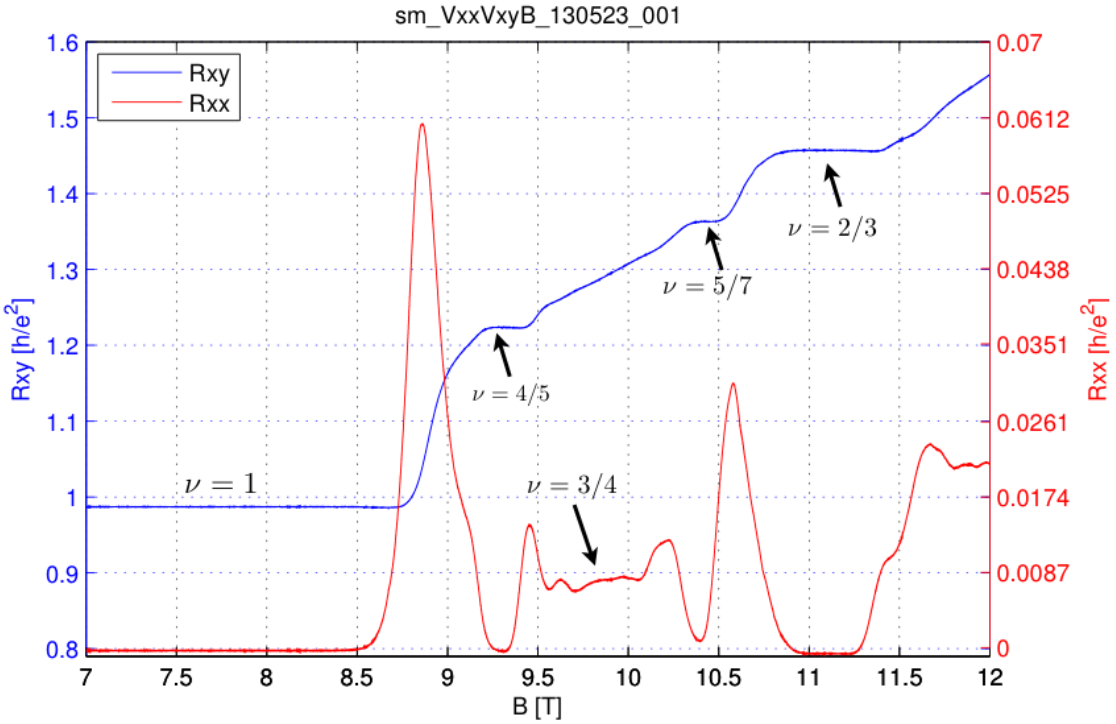

Figure 3.2: *Hall (blue) resistance and longitudinal (red) resistance as a function of magnetic field. The large plateau from 7 T to 8.7 T is $\nu = 1$, the plateau around 11 T is $\nu = 2/3$. Data from mesa C2 on WC2-P2-22-10.1*

temperature dependent plateaus and compare them to another sweep were the temperature is known. The most sensitive plateaus are the ones between $\nu = 2$ and $\nu = 3$, this region is home to $\nu = 5/2$ and the re-entrant IQH (RIQH) plateaus. According to [13] the RIQHE is caused by a non-uniform landscape of filling factor regions. The plateaus between $\nu = 2$ and $\nu = 3$ will not show up unless the 2DEG temperature is $\sim$ 20 mK and their shape will change dramatically as the temperature is lowered, from a rounded peak/dip to a real plateau-like shape.

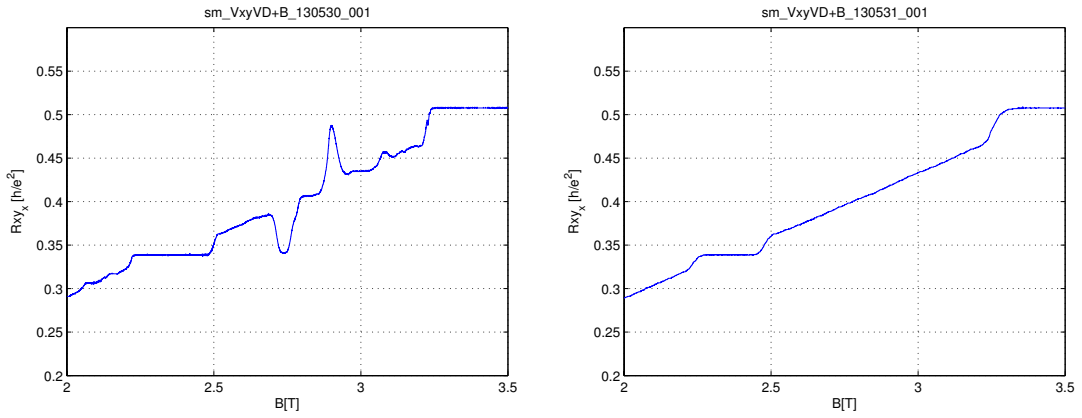

Figure 3.3: *The RIQH plateaus and $\nu = 5/2$ are very sensitive to temperatures below 20 mK. The left plot shows a sweep with an estimated temperature between 15 mK and 20 mK and the right plot shows a sweep with an estimated temperature above 30 mK. Data from mesa A2 on WC2-P2-22-10.1*

If there are no prior data with known temperature, one can still roughly estimate the 2DEG temperature from the shape of the RIQH plateaus. In figure 3.3 two different sweeps are shown (it should be noted that these measurements are done on the same chip as the data shown in figure 3.1 and figure 3.2, but on a different mesa), one with an estimated temperature between 15 mK and 20 mK and the other with an estimated temperature above 30 mK. The only difference in these two sweeps is the sweep rate and the sweep direction. The cold sweep was measured using a sweep rate of 10 mT/min and the magnet was swept from 12 T to 0T. In the hot sweep, the rate used was 30 mT/min and the magnet was swept from 0 T to 12 T. Apart from the sweep rate, the sweep direction also play a role, because of nuclear demagnetization in the copper pieces, in the fridge. In the discussion above it is seen that the 2DEG temperature is important for FQH measurements and proper heat sinking and low sweep rates are therefore essential. The temperature estimates in figure 3.3 are based on figure B.8 in [4].

Chapter 4

Conclusion and Outlook

Through the process described in this thesis we have successfully managed to reach electron temperatures on the order of 15 mK to 20 mK, low enough to see very temperature sensitive QH states like $\nu = 5/2$ and some RIQH states between $\nu = 2$ and $\nu = 3$. This was achieved by producing and installing new loom, bobbins and sapphire heat sinks. We found that a combination of low bias current and slow ramp rate of the magnet is essential if these temperature sensitive states are to emerge. In addition to a low bias current and a slow ramp rate it is also important to use a low lock-in frequency, in order to avoid a negative slope of R_{xx}. An important step on the way to our presented data was to realize that usage of high capacitance lines for ohmics will introduce a big out of phase signal, which seems to mix Hall and longitudinal resistances.

Having achieved such a low electron temperature has opened a wide range of possibilities for investigating different FQH-phenomena. As a start we wish to confirm or refute the findings of A. Kou et al [14]. They found that the quasiparticles emerging when moving away from the $\nu = 2/3$ plateau has charge $2e/3$ and that all charge is transported in a single edge.

Appendix A

Sapphire heat sink recipe

Obtain a sapphire wafer of size 40 mm x 25.5 mm x 0.5 mm, produced by Boston Piezo-Optics. Crystal orientation doesn't matter. Available surface finishes are polished (smooth) and fine-lapped (rough). Fine-lapped surfaces seem to promote better adhesion than polished ones, so we generally use a fine-lapped surface for the side with the traces, and a polished surface for the other side.

1. Clean the sapphire substrate by sonicating for 5 min each in Millipore water, Acetone, Methanol and then IPA. Blow dry with N_2.
2. Ash for 60 s and bake for 2 min at 185°C.
3. Evaporate 10/150 nm of Cr/Au on the rough side of the wafer using the AJA evaporation system (where the meanders will go).
4. Clean again as above (Step 1).
5. Bake 5 min at 185°C. Spin S1813 photoresist for 45 s at 5000 rpm. Bake for 2 min at 115°C.
6. Align photomask and expose for 10 s. (The intensity was $12.9 mW/cm^2$)
7. Develop using CD-26 and Millipore water: Sonicate for 40 s in CD-26 and rinse in Millipore water for 20 s. Blow dry with N_2.
8. Ash for 30 s.
9. If there is any edge bead that will leave some of the bond pads shorted together after etching, remove it now by exposing the edge. If you accidentally remove too much resist near the etch, you can patch it with a Sharpie (maker).
10. Etch gold layer, using Standard Gold Etchant[1], with an etch rate of 28 Å/s at room temperature. Etch for 56 s.
11. Rinse in Millipore water.
12. Etch the chromium layer using Chromium Etchant[2], with an etch rate of 40 Å/s at room temperature. Etch for 3 s.

[1] From Sigma-Aldrich
[2] From Sigma-Aldrich

13. Rinse in Millipore water. Inspect traces for any shorts or breaks. If there are breaks and you want to start over, you can wash off the resist and etch away the metal. If there are shorts because of excessive resist, remove the excess patches of resist and re-etch.

14. Remove resist thoroughly by soaking in acetone for 10 mins. Rinse in IPA and then blow dry with N_2.

15. Anneal in RTP at 530°C for 100 s using forming gas atmosphere.

16. Clean agian (Step 1).

17. Evaporate 10/200 nm of Cr/Au on the smooth side of the wafer, using the AJA evaporation system.

If you are worried about scratching the meander pattern in step 16 you can instead evaporate Cr/Au on the backside as the in step 17 as the first evaporation step. You then need to spin a layer of resist on the backside just before etching (you don't have to bake the resist, just leave it for 5 min to dry). As an alternative you can also cover your meander pattern with a layer of resist which you then remove with acetone after evaporating on the backside of the wafer.
When sonicating use a beaker that will allow the sapphire to lie horizontally to avoid cracks.

Appendix B

Wafer - P2-22-10.1

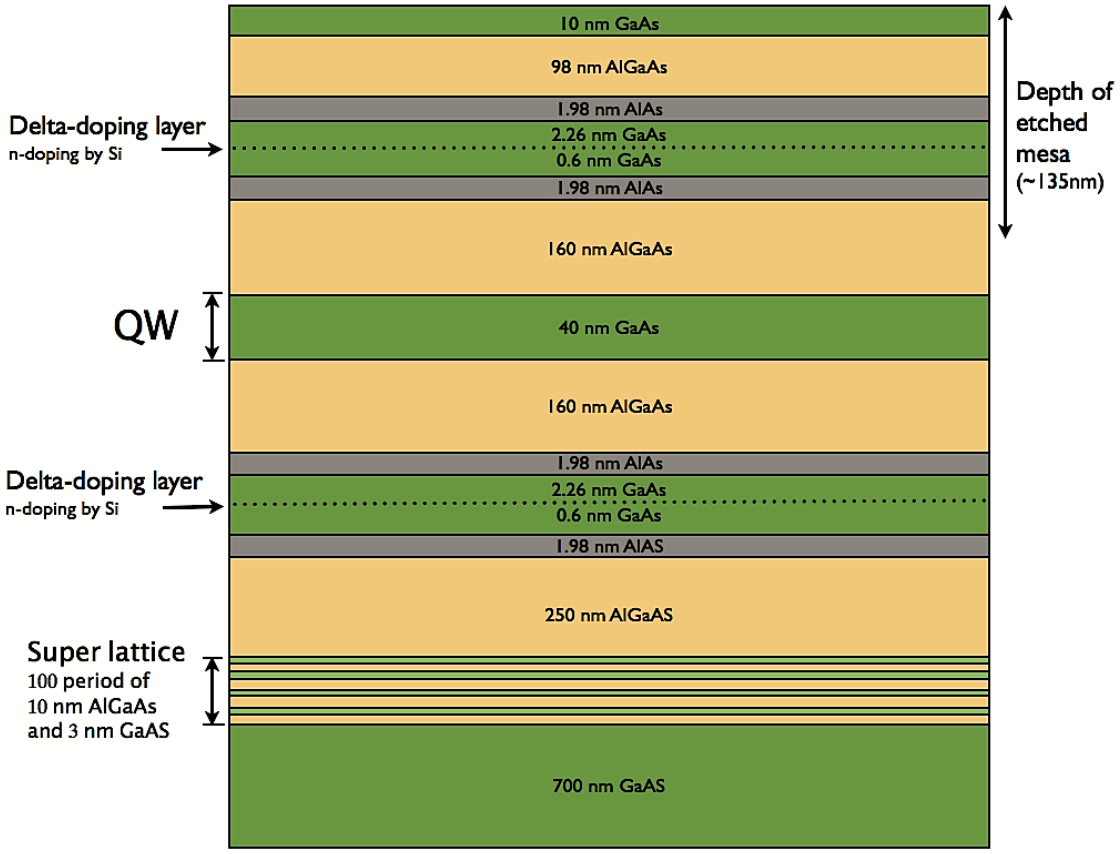

Figure B.1: *The structure of the wafer, grown by L. N. Pfeiffer, our mesa is fabricated on. Illustration is constructed from wafer data sheet 2-22-10.1*

Appendix C

The effect of high capacitance

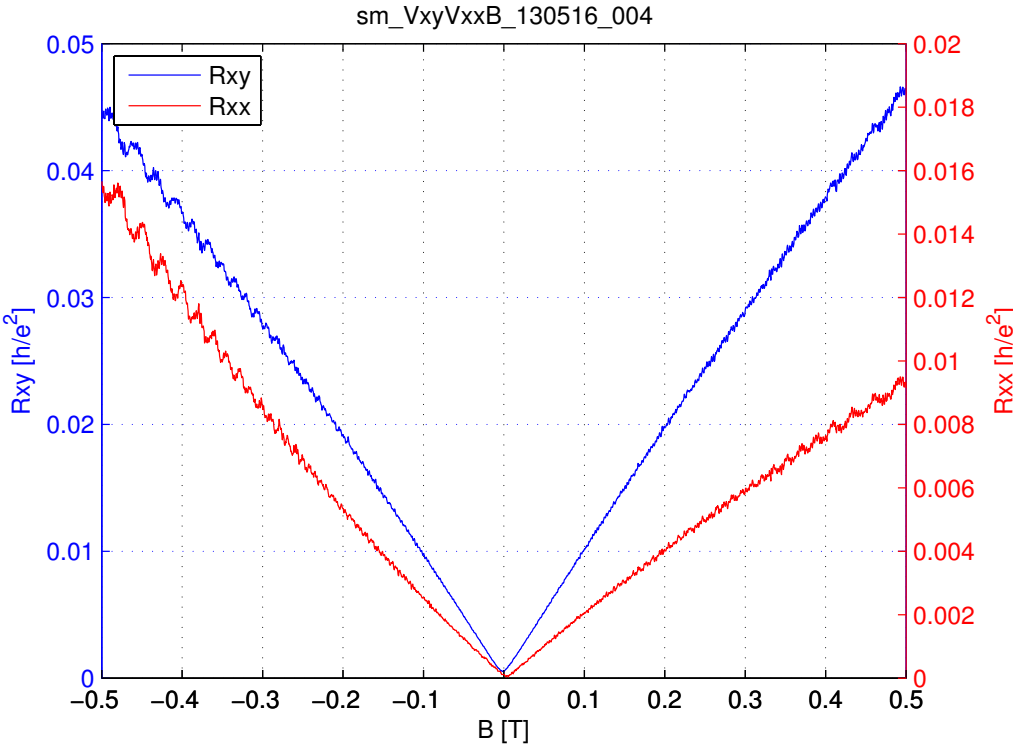

Figure C.1: *The measured R_{xy} signal is symmetric and behaves like we expect. The R_{xx} signal should have shown symmetric Shubnikov-de Haas oscillations around zero field. Instead we see a signal much more like R_{xy}, which indicate a mixing of the two signals. We don't see this mixing of signals when using small capacitors.*

Appendix D

Solidworks design file

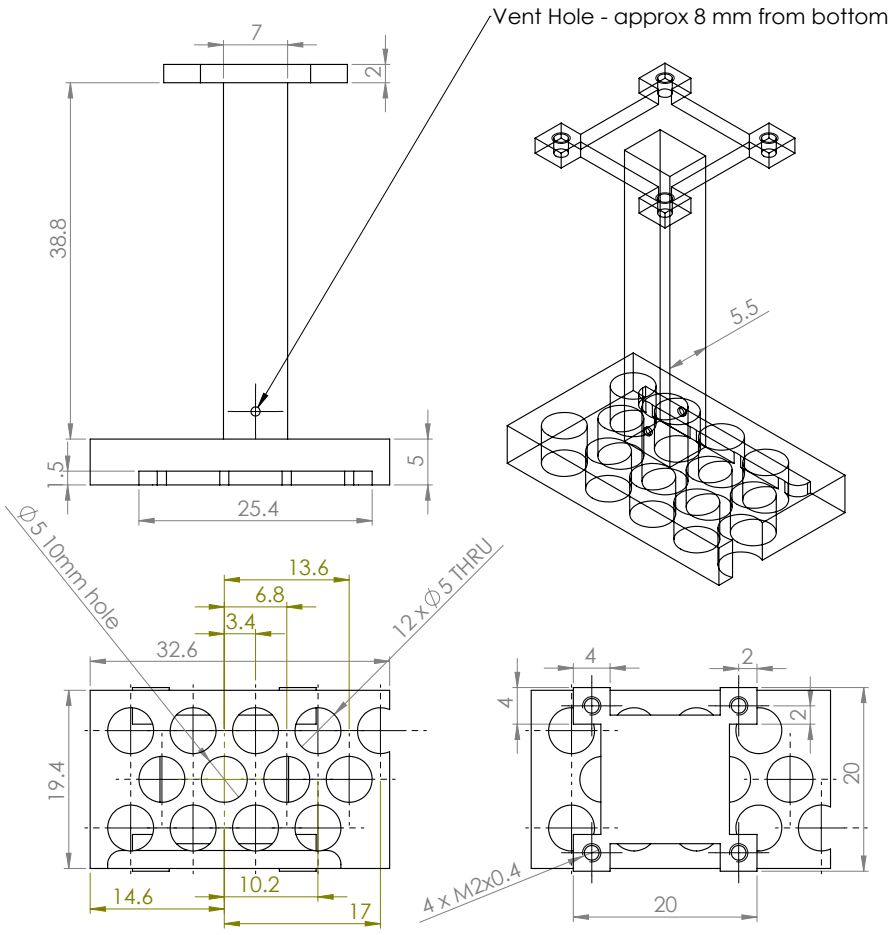

Item: FQHE Mount	Date: 05/10-12	Contact: Ferdinand Kuemmeth, kuemmeth@nbi.dk, +4521162657 Christian Olsen, chrede@me.com, +4561774499 Katrine Rasmussen, Kr_89@hotmail.com, +4561302744	
Material: OFHC Copper (provided)	Center for Quantum Devices		
Quantity: 1	Project: #35435		
	File: FQHE051012.sldprt		

Bibliography

[1] Horst L. Stormer. Nobel lecture: The fractional quantum hall effect. Reviews of Modern Physics, 71(4), July 1999.

[2] Charles Kittel. Introduction to Solid State Physics. John Wiley & Sons, Inc, 2005.

[3] Thomas Ihn. Semiconductor Nanostructures. Oxford University Press, 2011.

[4] Douglas Templeton McClure III. Interferometer-Based Studies of Quantum Hall Phenomena. PhD thesis, Harvard University, 2012.

[5] Jeno Solyom & Attila Piroth. Fundamentals of the Physics of Solids. Springer, 2008.

[6] Jainendra K. Jain. Composite Fermions. Cambridge University Press, 2007.

[7] Oxford Instruments. Triton 200 Cryofree Dilution.

[8] Guy K. White & Philip J. Meeson. Experimental Techniques in Low-Temperature Physics. Oxford University Press, 2002.

[9] Christian Enss & Siegfried Hunklinger. Low-Temperature Physics. Springer, 2005.

[10] Robert C. Richardson & Eric N. Smith. Experimental Techniques In Condensed Matter Physics At Low Temperatures. The Advanced Book Program, 1988.

[11] Henry W. Ott. Noise Reduction Techniques In Electronic Systems. John Wiley & Sons, Inc, 1988.

[12] Stanford Research. SR830 DSP Lock-in Amplifier.

[13] M. M. Fogler et al. Ground state of a two-dimensional electron liquid in a weak magnetic field. Physics Review B, 54(1853), 1996.

[14] A. Kou et al. Coulomb oscillations in antidots in the integer and fractional quantum hall regimes. Physical Review Letters, 108(256803), 2012.